

Detect and Pointing Algorithm's Performance for a Planar Smart Antenna Array: A Review

Tiago Varum^{1,2}, João N. Matos^{1,2}, and Pedro Pinho^{2,3}

¹ Departamento de Engenharia Eletrónica, Telecomunicações e Informática
Universidade de Aveiro, Aveiro, Portugal

² Instituto de Telecomunicações
Campus Universitário de Santiago, Aveiro, Portugal

³ Instituto Superior de Engenharia de Lisboa, Lisboa, Portugal
tiago.varum@ua.pt, matos@ua.pt, ppinho@deetc.isel.pt

Abstract — An adaptive antenna array combines the signal of each element, using some constraints to produce the radiation pattern of the antenna, while maximizing the performance of the system. Direction of arrival (DOA) algorithms are applied to determine the directions of impinging signals, whereas beamforming techniques are employed to determine the appropriate weights for the array elements, to create the desired pattern. In this paper, a detailed analysis of both categories of algorithms is made, when a planar antenna array is used. Several simulation results show that it is possible to point an antenna array in a desired direction based on the DOA estimation and on the beamforming algorithms. A comparison of the performance in terms of runtime and accuracy of the used algorithms is made. These characteristics are dependent on the SNR of the incoming signal.

Index Terms — Adaptive antenna array, beamforming, direction of arrival, planar array.

I. INTRODUCTION

The adaptive or smart antennas due its benefits have a great potential over all the future wireless communications. These antennas consist of arrays with several elements, which combines the received data from each element of array in such a way that improves the communication, suppressing interfering signals.

The increase of the coverage, the enhancement of the system capacity and the ability to reduce/mitigate some communication impairments such as interferences and multipath fading are relevant features about the impact of this technology in the performance of the wireless communications. The smart antennas has the spatial diversity capabilities, which relies in the possibility to transmit simultaneously several data streams, exploiting the spatial multiplexing gain of

MIMO systems, increasing the spectral efficiency and the data rates.

Firstly developed for military applications, in the last century, took part the evolution of wireless communications and, nowadays, the smart antennas are attractive for several areas that range from the military applications, satellites, and mobile communications, especially in base stations, 4G MIMO and the emerging 5G MIMO.

The adaptive antennas can detect the direction of signals that impinge at the antenna using the direction of arrival estimation algorithms, and then weighting each array element can change the radiation pattern of the antenna, not only to point to a preferred zone, but also to place nulls in the others, to mitigate possible interfering signals.

These weights (amplitude and phase) are estimated using the beamforming algorithms. The block diagram of a smart antenna procedure is presented in the Fig. 1. In reception mode, a sample of received signal at each element of the array is used through DOA algorithms to estimate the directions of the arriving signals. Once determined, the directions of interest and of the interfering signals are selected, by some auxiliary intelligence. Then, using the angular locations, the beamforming algorithms are used to compute the needed weight to apply to each element of the array, to point the antenna pattern as is intended.

This paper is organized into six sections. It starts with an introduction, inserting the work in the smart antenna domain. The second section describes the direction of arrival estimation algorithms, with a focus in the two dimensional antenna arrays. The following section, the third, is related to beamforming, exposing the main algorithms applied into planar smart antennas. In the fourth section is made the system integration, combining the DOA and beamforming algorithms to

create an example of application, detecting signals and pointing the radiation pattern of a planar array antenna for them. Then, there is a section of results with a detailed examination of the performance of the algorithms. Finally, the paper is concluded in the section six, grouping the main results taken from this analysis and some future prospects.

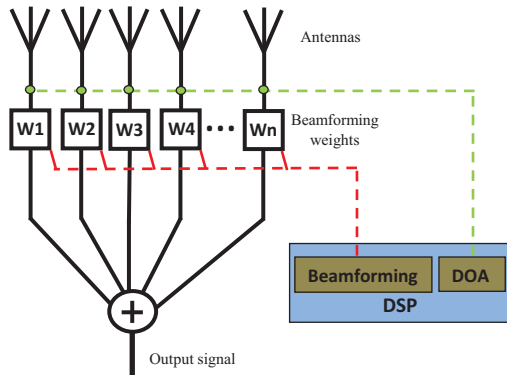


Fig. 1. Adaptive antenna array system.

II. DIRECTION OF ARRIVAL

The algorithms to determine the directions of arrival of the signals are a vital part of the adaptive antenna system, due to its ability to filter out the surrounding noise.

Processing the electromagnetic waves that reach to the antenna array is possible to extract some info about the signal, such the direction whence is arriving to the antenna. Estimating the DOA's, then is possible to distinguish the directions of interest to point the antenna and directions of intrusive signals, to reduce its effects in the communication.

There are three classes of methods to do this, the classical, the maximum likelihood and the subspace methods, which differ mainly in the performance and computational requirements [1], [2]. The classics are based in the beamforming, in which the central idea is to scan the antenna beam over the space and the locals in which more power is received are the DOAs. These methods are theoretically simple but involve a high computational effort and offer a low performance. A different class is based on the maximum likelihood techniques, which present a high performance but with high computational requirements, due to the necessity to solve nonlinear multidimensional optimization problems. Finally, the subspace methods make use of the received signal and noise subspace to achieve a tradeoff between the performance and the computational efficiency. The performance of the subspace-based methods is limited essentially by the accuracy of distinguishing the signal and the noise subspaces in the presence of noise. For the planar uniform array the most applied algorithms are MUSIC and the 2D ESPRIT, that are subspace based [1].

A. Multiple signal classification - MUSIC algorithm

This DOA algorithm is perhaps the most popular method and uses the fact that the steering vectors of the incoming signals lie in signal subspace and are orthogonal to the noise subspace. The MUSIC [2]-[5] search in the all possible steering vectors, those that are orthogonal to the noise subspace of the covariance matrix of the received data.

Using the received information from each array element, the MUSIC through eigenvalue decomposition or singular value decomposition of the correlation matrix of this data, estimates the noise subspace, as exemplified in the diagram of Fig. 2. After the noise subspace be known, U_N , the DOAs are the resulting peaks of the MUSIC spectrum, that is given by equation (1), that is function of θ and φ through the steering vector $s(\theta, \varphi)$:

$$P_{MUSIC}(\theta, \varphi) = \frac{1}{s^H(\theta, \varphi) U_N U_N^H s(\theta, \varphi)}, \quad (1)$$

where M^H represents the conjugate transpose matrix of M (Hermitian). When a steering vector is referring to one arriving signal, the product $s^H(\theta, \varphi) U_N$ is equal to zero, ideally, and the function assumes a high value (peak).

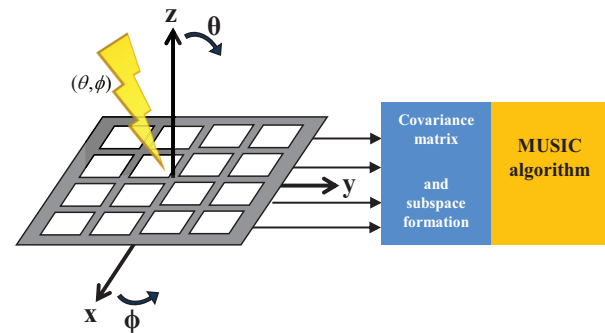


Fig. 2. 2D MUSIC.

The MUSIC algorithm is easily understood and can be implemented in all antenna array geometries, however, computationally requires a lot of resources, since it should calculate the MUSIC spectrum, equation (1), for all possible steering vectors to estimate the desired peaks. The estimation error of MUSIC algorithm is substantially influenced by the angle grid interval in which the equation (1) is evaluated.

In the presence of coherent signals, as in multipath environments, spatial smoothing schemes [6], [7] must be applied to suppress the correlations between the incoming signals.

B. Estimation of signal parameters via rotational invariance techniques - 2D ESPRIT algorithm

An additional known subspace based DOA algorithm is the ESPRIT [8]-[12]. This scheme solves

the issues of the high computational requirements of the MUSIC, and the resulting effects of array calibration errors. The ESPRIT algorithm employs the property of shift invariance of the antenna array, and due to this property is not fundamental to have a high level of calibration in the array.

The computational complexity of the ESPRIT is reduced once this algorithm imposes some constraints on array structure. The ESPRIT assumes that the separation between equivalent elements in each sub-array is fixed, Fig. 3, and therefore the array presents a translational invariance. This translational invariance leads to a rotational invariance of the signal subspace that will allow estimating the DOAs.

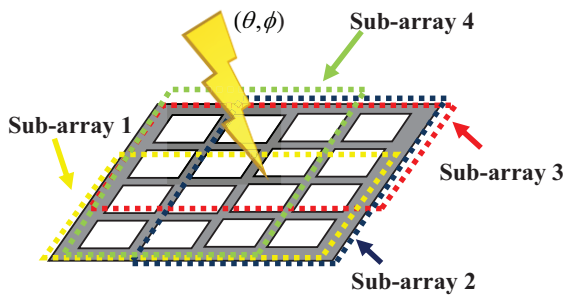


Fig. 3. Sub-array division (3x4) with maximum overlap.

The algorithm follows three steps, the signal subspace estimation, the solution of the invariance equation and the DOA estimation.

1) *Signal subspace estimation:*

$$\text{Computation of the } U_s. \quad (2)$$

2) *Solve the invariance equation:*

$$\begin{aligned} K_{u1}U_s Y_u &= K_{u2}U_s, \\ K_{v1}U_s Y_v &= K_{v2}U_s, \end{aligned} \quad (3)$$

where K_{u1} , K_{u2} , K_{v1} and K_{v2} represent the two pairs of transformed selection matrices, while Y_u and Y_v are the real-valued matrices [10].

3) *DOA estimation:*

$$\begin{aligned} \lambda_i \quad i=1 \dots d &\rightarrow \text{eigenvalues of } Y_u + jY_v, \\ u_i &= 2 \tan^{-1}(\text{Re}\{\lambda_i\}), \\ v_i &= 2 \tan^{-1}(\text{Im}\{\lambda_i\}), \\ \varphi_i &= \arg(u_i - jv_i) \quad \theta_i = \sin^{-1}(\|u_i - jv_i\|), \end{aligned} \quad (4)$$

where θ_i and φ_i are the DOA angular information.

III. BEAMFORMING

In fact, despite the interest and intrusive signals occupying the same frequency range, they are created from different spatial positions. Once identified the directions of arrival of its signals, is necessary the use of spatial filtering techniques, also known as beamforming techniques, due to deal with in the beam pattern of an

antenna array. Based on these directions, the beamforming processing to control the antenna pattern is made, improving the performance of the communication.

The control of the radiation pattern of the antenna array is achieved, as is illustrated in the Fig. 4, varying the relative amplitude and phase of each element of the array and is based on this rule that the beamforming techniques operate. There are several algorithms already developed to calculate the complex weights (amplitude and phase) to apply to the antenna array.

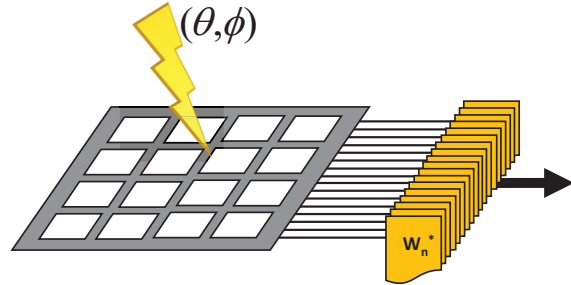


Fig. 4. Beamformer system.

These beamforming techniques can be classified according to the way on how the weights apply to the array are estimated, as data independent or statistically optimum [13], [14]. In the data independent, the weights are chosen to provide a desired response independently of the received data by the antenna, while in the statistically optimum the weights are estimated according to the statistics of the received signal in order to optimize its response, reducing or ideally suppressing the intrusive signals.

Often, statistical information of the collected data from the array are not available or varies in time, therefore adaptive algorithms are typically useful to estimate the weights and are designed in order to their response tend to a solution statistically optimum.

A. Statistically optimum beamformer

These beamformers are applied to diminish the influence of the interfering signals in the communication while pointing the antenna pattern in the direction of interest signal. Some examples of statistically optimum algorithms present in the literature [13] are:

- Multiple sidelobe canceller (MSC),
- Use of reference signal,
- Maximum SNR,
- Linearly constrained minimum variance (LCMV).

The MSC beamformer is composed by a main channel and others auxiliary channels, and the idea is to choose the appropriate weights to apply to the auxiliary channels to cancel the interference signals from the main channel. This procedure presents some limitations, once MSC doesn't point the main beam to a desired signal,

and the weights must be estimated with the absence of the desired signal. Based on this, MSC is only effective when desired signals are weak relative to interferences. The use of a reference signal requires some knowledge about the desired signal, to generate a reference signal in order to minimize the mean square error between the output and the reference signal. Using the maximum SNR solution requires the knowledge of the covariance matrix of the desired signal and of the noise.

Finally, one of the most important statistically optimum algorithms with higher applicability is the LCMV, which is described below followed by a different approach of its formulation known as generalized side lobe canceller (GSC).

1) Linearly Constrained Minimum Variance

Most of the times the desired reference signal is unknown or we don't have enough information about it, being necessary to impose some linear constraints in the weight vector to minimize the variance of beamformer output. This is obtained using the LCMV beamformer [15]. The constraints impose that the desired signals from a known direction are preserved and the interfering signals influence is minimized.

The LCMV formulation problem is to select the complex weights that are suitable to the multiple linearly independent constraints:

$$\min_w w^H R_x w \quad \text{subject to} \quad C^H w = f, \quad (5)$$

where w is the vector of weights, R_x the covariance matrix, C is the constraint matrix and f is the response vector.

The solution of the constrained minimization of LCMV problem can be achieved applying the method of Lagrange multipliers and results in [13]:

$$W_{opt} = R_x^{-1} C (C^H R_x C)^{-1} f. \quad (6)$$

It is important to note the dependence of the optimal weight vector (6) with the data correlation matrix, and therefore with the statistics of the input signal.

a) Generalized Sidelobe Canceller - GSC

The generalized sidelobe canceller is a different approach to solve the LCMV problem, providing a simple implementation of the beamformer and change the constrained minimization problem to an unconstrained scheme [16], [17].

The GSC separates the LCMV problem into two components, one data independent and other data dependent, as is illustrated in Fig. 5. In GSC structure, the optimum weight vector is decomposed in two orthogonal components that are in the range and null space of C , in the manner that $w = w_o - B w_M$. The array output is $y = w_o^H x - w_M^H B^H x$, as is shown in the Fig. 5.

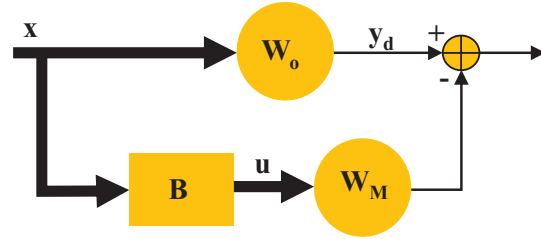


Fig. 5. Generalized sidelobe canceller.

The w_o vector is the quiescent part of w , and is used to constrain the weight subspace, and must satisfy the linear constraints [16]:

$$C^H w_o = f \Rightarrow w_o = C (C^H C)^{-1} f. \quad (7)$$

The w_o is designed respecting the imposed restrictions, is independent of the data and represents the non-adaptive component of the LCMV solution. In inferior branch, the blocking matrix B and w_M will block the interfering signals influence, while minimizing the variance of the output signal y . This is the data dependent component. The blocking matrix B must be orthogonal to the constraint matrix C , so $C^H B = 0$.

The GSC unconstrained problem is:

$$\min_{w_M} (w_o - B w_M)^H R_x (w_o - B w_M), \quad (8)$$

subject to $C^H w = f$,

and the optimal solution is:

$$w_M = (B^H R_x B)^{-1} B^H R_x w_o. \quad (9)$$

This implementation of beamformer has significant benefits, such the w_o is a data independent beamformer and w_M is an unconstrained beamformer.

B. Adaptive algorithms

The statistically optimum beamformers uses the received data statistics, which often may change over the time or may not be available. Adaptive algorithms solve this issue [13].

The adaptation error corresponding to a weight vector is calculated and then is processed a new weight vector with a reduced error. Examples of adaptive algorithms are the well-known least mean square (LMS), the recursive least squares (RLS) or the Frost's algorithm.

1) Frost's Algorithm for LCMV Beamforming

The Frost's algorithm [14] belongs to the group of LCMV beamformers. The LCMV estimated weights are based on the received data information statistics (R_x), but in many situations the second order statistics are not available or are continuously changing, being necessary the use of adaptive algorithms. Frost's algorithm solution minimizes the mean square error while

maintains the specified response to the desired signal. The weight vector starts with an initial value:

$$w = C(C^H C)^{-1} f, \quad (10)$$

and in each iteration the vector will be updated on negative gradient direction by a factor defined by μ :

$$\begin{aligned} w(n+1) &= C(C^H C)^{-1} f + P(w(n) - \mu e^*(n)x(n)), \\ P &= I - C(C^H C)^{-1} C^H. \end{aligned} \quad (11)$$

2) Least Mean Square

Least mean square algorithm [13], [14], [18], [19] estimates the gradient vector and adjusts the weight vector in the negative gradient direction at each iteration:

$$\begin{aligned} w_M(n) &= w_M(n-1) + \mu u(n-1)y^*(n-1), \\ y(n) &= y_d(n) - w_M^H(n)u(n), \\ 0 < \mu < \frac{1}{\lambda_{\max}}, \end{aligned} \quad (12)$$

where λ_{\max} is the largest eigenvalue of the correlation matrix.

The gain μ [13] ($0 < \mu < 1$) is the parameter that controls the convergence rate. Smaller values result in slow convergence and good approximation, while higher values lead to faster convergence and the stability around the minimum value is not guaranteed. This is a simple algorithm and with a correct choice value of μ , the weight vector tends to an optimum solution.

3) Recursive Least Squares

The recursive least squares [13], [14] has a high convergence rate, faster than the LMS; however, the computational complexity is higher.

The RLS problem is:

$$\min_{w_M(k)} \sum_{n=0}^N \lambda^{N-n} |y_d(n) - w_M^H(n)u(n)|^2, \quad (13)$$

with $0 < \lambda < 1$ a constant called forgetting factor.

The algorithm can be described as [13]:

$$\begin{aligned} P(0) &= \delta^{-1} I, \\ v(n) &= P(n-1)u(n), \\ k(n) &= \frac{\lambda^{-1} v(n)}{1 + \lambda^{-1} u^H(n)v(n)}, \\ \alpha(n) &= y_d(n) - w_M^H(n-1)u(n), \\ w_M(n) &= w_M(n-1) + k(n)\alpha^*(n), \\ P(n) &= \lambda^{-1} P(n-1) - \lambda^{-1} k(n)v^H(n), \end{aligned} \quad (14)$$

where I is the identity matrix and δ a small value.

IV. SYSTEM INTEGRATION

The simulated system consists of a planar antenna array that receives an input signal $x(t)$, that is a sum of various signals impinging in the antenna and noise, as is shown in the Fig. 6. The received data is after processed

to estimate the angles of arrival of each signal. Then, using the beamforming algorithms, the system processes the group of weights to apply to each antenna array element to point the radiation pattern to the desired direction while minimizing the impact of the others signals considered as interferences.

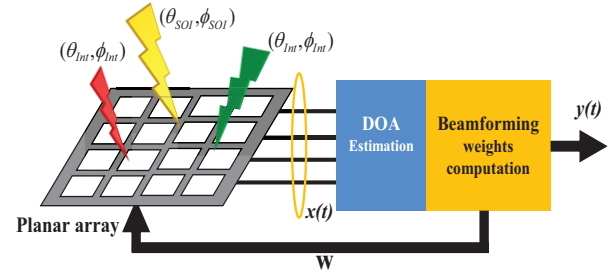


Fig. 6. Implemented system.

Consider a $M \times N$ uniform planar array as presented in the Fig. 7, with spacing between elements of d_1 on rows and d_2 on columns. There are J signals $s_i(t)$ that collide onto the antenna array with an elevation angle θ and with an azimuth angle ϕ . The input signal at each array element (m, n) is the sum of the contributions of the J signals and noise $n(t)$:

$$x_{nm}(t) = \sum_{i=1}^J s_i(t) e^{j \frac{2\pi}{\lambda} [u_i d_1 (m-1) + v_i d_2 (n-1)]} + n_{nm}(t) \quad (15)$$

$$u_i = \sin \theta_i \quad v_i = \cos \theta_i \sin \phi_i$$

$$m = 1, \dots, M \quad n = 1, \dots, N \quad i = 1, \dots, J,$$

where λ is the wavelength.

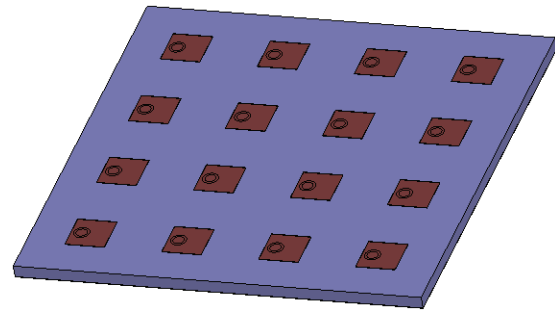


Fig. 7. Planar array.

It is possible to represent the received data in vector structure $X(t)$ and noise vector $N(t)$ as:

$$X(t) = [x_{11}(t) \ x_{21}(t) \ \dots \ x_{N1}(t) \ x_{12}(t) \ \dots \ x_{MN}(t)]^T, \quad (16)$$

$$N(t) = [n_{11}(t) \ n_{21}(t) \ \dots \ n_{N1}(t) \ n_{12}(t) \ \dots \ n_{MN}(t)]^T. \quad (17)$$

The steering vector of the each signal that arrives to the planar array contains the set of phase delays that a wave will take relating to each element of the array, and for a planar array can be represented as [20], [21]:

$$C_u = \begin{bmatrix} 1 & e^{j\frac{2\pi d_1}{\lambda}(2-1)u_1} & \dots & e^{j\frac{2\pi d_1}{\lambda}(M-1)u_1} \end{bmatrix}^T, \quad (18)$$

$$C_v = \begin{bmatrix} 1 & e^{j\frac{2\pi d_2}{\lambda}(2-1)v_1} & \dots & e^{j\frac{2\pi d_2}{\lambda}(N-1)v_1} \end{bmatrix}^T, \quad (19)$$

$$A = C_u \otimes C_v, \quad (20)$$

where the \otimes is the Kronecker product, C_u and C_v are the steering vectors in x and y direction and A the steering matrix of the planar antenna array.

So, the total input signal $X(t)$ can be expressed in the following formula:

$$X(t) = \sum_{i=1}^J s_i(t) A_i + N(t). \quad (21)$$

The output signal of the planar array, with beamforming weights W applied to each array element will be:

$$y(t) = W^H X(t), \quad (22)$$

$$W = [w_{11} \ w_{21} \ \dots \ w_{N1} \ w_{12} \ \dots \ w_{MN}]. \quad (23)$$

In this work, the signal $X(t)$ that collides to the planar array antenna is generated previously. This data is the sum of diverse signals with different directions (θ, φ) , the signal of interest, interferences and noise.

The set of signal samples that reaches each element of the array is processed by a DOA algorithm to determine the angles of arrival and the number of signals.

With some knowledge to distinguish the interest signal and interferences, one of beamforming algorithms is applied to achieve the correct weights to point the antenna array to the desired location.

The antenna array for test presented in the Fig. 7, was simulated in the electromagnetic simulator HFSS (High Frequency Structure Simulator) [22] and consists of a planar microstrip array of 16 elements with a 4x4 shape, designed for 12 GHz.

Using as a uniform planar antenna array, that uses all elements feed with the same amplitude and phase (unitary weights), the radiation pattern of the antenna is perpendicular to the antenna plane, and points to the origin $(\theta, \varphi) = (0^\circ, 0^\circ)$.

In the electromagnetic simulator is possible to modify the relative amplitude and phase of each element of the array, based on this, the calculated weights with beamforming algorithms were tested in the simulated planar antenna array.

V. RESULTS

Using the MATLAB [23], the DOA and beamforming algorithms were implemented and its performance was analyzed when applied to a planar antenna array. The system (DOA and beamforming) simulation was tested using several group of angles of

arrival of signals with excellent results. As an example of test, two signals with directions $(\theta, \varphi) = (45^\circ, 45^\circ)$ and $(\theta, \varphi) = (70^\circ, 0^\circ)$ was employed using a 4x4 planar antenna array with 0.5λ element spacing, as presented in Fig. 7.

A. Direction of arrival

With the received signal (16) from each element of the antenna array (that is a composite of various components of interest signals, interference signals and noise), the direction of arrival algorithms estimates the locals that electromagnetic signals are arriving to the antenna. The MUSIC and ESPRIT algorithms were tested.

a) MUSIC

The 2D MUSIC algorithm creates a two-dimensional grid, in the range which the angles vary $\theta \in [0, 90]$ $\varphi \in [0, 360]$, and then, evaluates the function P_{MUSIC} (1) for each point of the grid. The Fig. 8 illustrates the result of the MUSIC algorithm, a spatial graph that present peaks in the position of incident signals.

According to the Fig. 8, the function contains two peaks, which are evidenced. Note that there is another peak but is assumed to be repeated, once 0° and 360° is the same spatial location. To be easier to define the peaks of the graph, one function to detect correctly the N maxima values was implemented. This function only gives the points of zero gradient.

The result of this function is shown in the Fig. 9, with the two well defined peaks. The output of the MUSIC algorithm is that the incident signals that arrive to antenna are coming from $(45.3^\circ, 44.82^\circ)$ and $(70.07^\circ, 0^\circ)$, which are very close to the initially proposed angles.

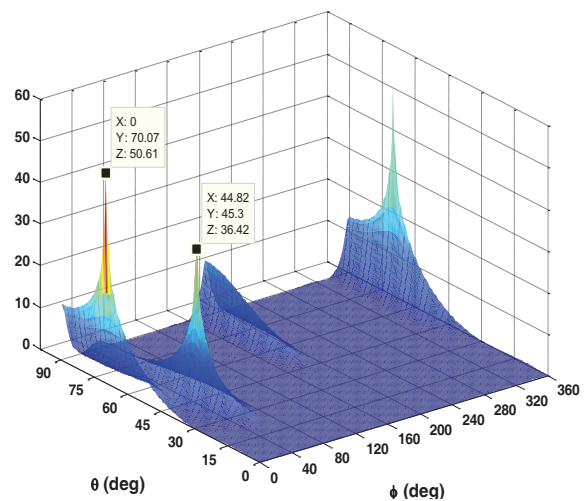


Fig. 8. 2D MUSIC spectrum.

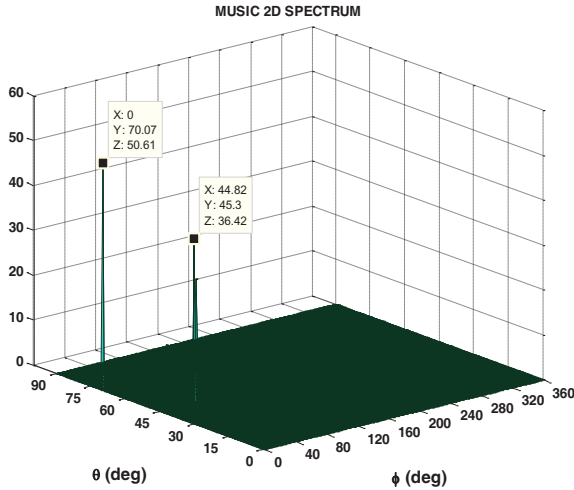


Fig.9. MUSIC 2D spectrum peaks.

b) *ESPRIT*

Using the equal received signal $X(t)$ by each element of the antenna was processed the other DOA estimator, the ESPRIT algorithm. This algorithm doesn't use a grid to evaluate a function, but the output is just the pair of angles (θ, φ) estimated.

The output of the ESPRIT algorithm estimates that the signals are arriving from $(\theta, \varphi) = (45.02^\circ, 45.11^\circ)$ and $(\theta, \varphi) = (69.82^\circ, 0.03^\circ)$.

The DOA algorithms implemented exhibit estimated results very approximate to the original values. These algorithms only receive the signal $X(t)$, and provides the spatial position of each incoming source which compose it.

Once known the DOA's of the signals, is necessary to apply some knowledge and choose the local to point the antenna and interfering directions. Assuming that the first pair of values (θ, φ) is the direction of interest, and the following the interfering signals, the system then employs the beamforming algorithms to determine the appropriate weights to apply to each element of the antenna array.

B. Beamforming

The beamforming weights are a set of amplitude and phase delays that are applied to an antenna array, to combine the signals in such way that produces constructive interference in some locals and destructive in others. These weights can be displayed in an exponential form $w = A e^{j\phi}$.

The four beamforming algorithms presented before were tested and the resulting weights were inserted in the simulated antenna of the Fig. 7 and evaluated the obtained radiation pattern. The locals (θ, φ) of the

considered signals are: signal of interest: $(45^\circ, 45^\circ)$, and interference: $(70^\circ, 0^\circ)$.

a) *LCMV*

The optimum solution for the LVCB problem were implemented, with input of the angles estimated by DOA algorithm, and using a response vector $f = [1 \ 0]^H$ to consider the first pair of angles the interest direction and the second the local of interference.

The result of the algorithm is presented in the Table 1, this output is composed by the complex weights already decomposed in terms of amplitude and phase, to apply directly to the corresponding element of the 4x4 array.

Table 1: Weights resulting from LCMV beamforming algorithm

Optimum LCMV				
Amplitude \angle phase				
	1	2	3	4
1	1.0 \angle 0°	1.0 \angle -90°	1.0 \angle -180°	1.0 \angle 90°
2	1.0 \angle -90°	1.0 \angle 180°	1.0 \angle 90°	1.0 \angle 0°
3	1.0 \angle 180°	1.0 \angle 89°	1.0 \angle 0°	1.0 \angle -90°
4	1.0 \angle 90°	1.0 \angle 0°	1.0 \angle -91°	1.0 \angle 180°

The resultant radiation pattern of the planar antenna with these weights applied is shown in the Fig. 10. It's possible to observe the maximum of the radiation pattern pointed to the local $(45^\circ, 45^\circ)$ of the signal of interest, with green dashed arrow, while in the direction $(70^\circ, 0^\circ)$, with a red filled arrow, exists a low power value to diminish significantly the influence of the interference signal in the received from this direction.

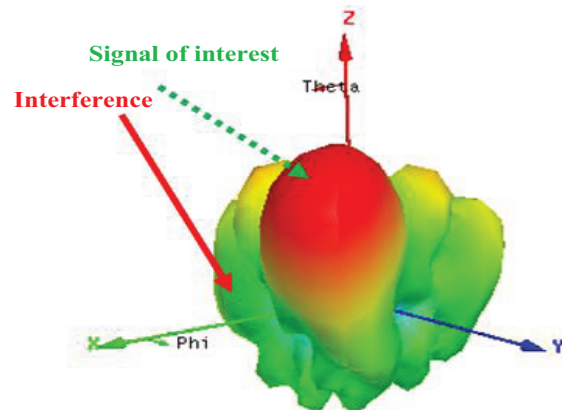


Fig. 10. The radiation pattern of the planar array with optimum LCMV weights applied.

b) *Adaptive Frost's Algorithm for LCMV Beamforming*

Another solution to solve the problem is using

adaptive algorithms that are a more realistic approach, due to the environment changes.

With the considered pair of angles for the signal of interest and interference directions, was tested the adaptive Frost's algorithm for LCMV beamforming. This algorithm was processed with a 100 samples of the input signal, iteratively, and the output resulting weights is presented in the Table 2.

Table 2: Weights resulting of adaptive Frost's algorithm for LCMV beamforming

Adaptive Frost's LCMV				
Amplitude \angle phase				
	1	2	3	4
1	1.0 \angle 0°	1.0 \angle -90°	1.0 \angle -180°	1.0 \angle 90°
2	1.0 \angle -90°	1.0 \angle -180°	1.0 \angle 90°	1.0 \angle 0°
3	1.0 \angle 180°	1.0 \angle 90°	1.0 \angle 0°	1.0 \angle -90°
4	1.0 \angle 90°	1.0 \angle 0°	1.0 \angle -90°	1.0 \angle -180°

With these weights applied in the planar antenna, the new radiation pattern created is presented in the Fig. 11. It's observed that the antenna points to the direction of interest (green dashed arrow) placing a null in the interference zone (red filled arrow), as is pretended.

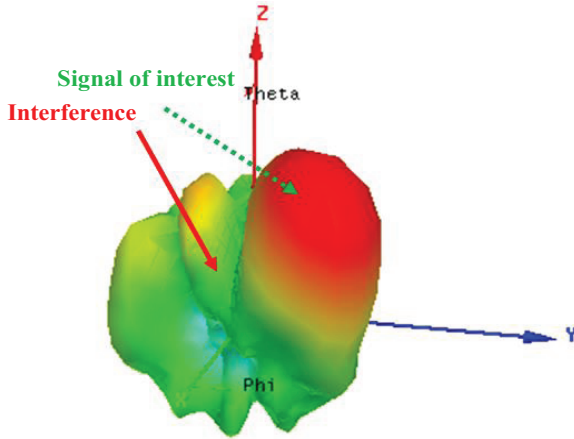


Fig. 11. The radiation pattern of the planar array with Frost's algorithm beamforming weights applied.

c) *LMS*

The known algorithm of least mean square was also performed in MATLAB, for a planar antenna array and to point to the considered directions. The result of this algorithm is available in the following Table 3.

This adaptive algorithm uses as the previous 100 samples of the received signal $X(t)$. The produced radiation pattern when inserted the LMS weights is illustrated in the Fig. 12.

As is visible, the antenna points its maximum (green dashed arrow) in the direction $(45^\circ, 45^\circ)$ and places a null

(red filled arrow) in the $(70^\circ, 0^\circ)$ zone.

Table 3: Weights resulting of the adaptive LMS beamforming algorithm

Adaptive LMS				
Amplitude \angle phase				
	1	2	3	4
1	1.0 \angle 0°	1.0 \angle -83°	0.9 \angle 156°	0.6 \angle 83°
2	0.7 \angle -83°	1.0 \angle 179°	1.0 \angle 93°	1.2 \angle 2°
3	0.9 \angle -178°	0.9 \angle 61°	0.9 \angle 23°	0.6 \angle -78°
4	0.9 \angle 69°	0.6 \angle 13°	0.6 \angle -59°	0.6 \angle -169°

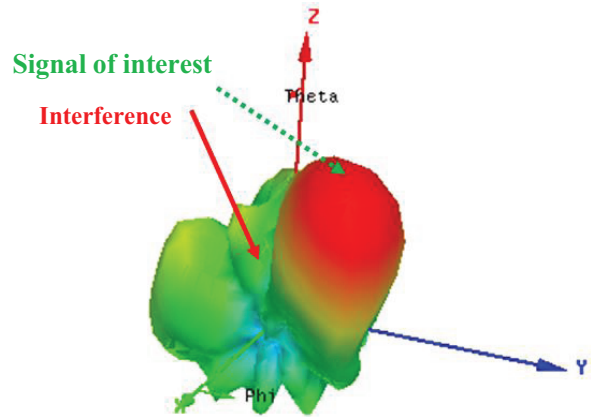


Fig. 12. The radiation pattern of the planar array with LMS algorithm beamforming weights applied.

d) *RLS*

The recursive least squares algorithm was also implemented to estimate the appropriate weights for this scenario. The output of this algorithm is presented in the Table 4, with the amplitudes and phases calculated to employ in the simulated antenna array.

Table 4: Weights resulting of the adaptive RLS beamforming algorithm

Adaptive RLS				
Amplitude \angle phase				
	1	2	3	4
1	1.0 \angle 0°	0.7 \angle -104°	0.5 \angle -161°	0.9 \angle 102°
2	1.2 \angle -92°	1.2 \angle 175°	0.8 \angle 107°	0.9 \angle -34°
3	0.8 \angle -163°	0.3 \angle 127°	0.8 \angle -100°	0.8 \angle -73°
4	0.4 \angle 101°	0.6 \angle -4°	0.7 \angle -114°	0.5 \angle -128°

With this set of weights applied in the array, leads to the resulting radiation pattern that is shown in the Fig. 13.

As expected, the antenna will move its radiation pattern in the direction of interest $(45^\circ, 45^\circ)$ indicated by green dashed arrow, becoming profitable the communication with a signal from this direction.

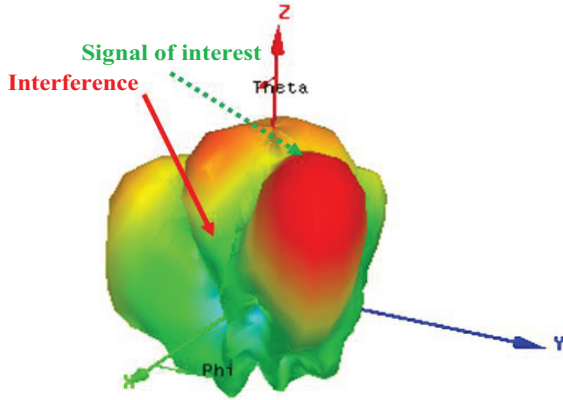


Fig. 13. The radiation pattern of the planar array with RLS algorithm beamforming weights applied.

After the estimation of the arrival directions of the impinging signals to the antenna and the calculation of the weights to steer the radiation pattern, using various algorithms, it is imperative a comparative description about their performance.

C. System performance

The system that consists of DOA estimation and computation of the beamforming weights was evaluated. The performance can be evaluated in terms of running time for all algorithms, the changeability of its results when the noise level alters and in terms of estimation errors.

Varying the signal to noise ratio (SNR), the runtime of the all algorithms was analyzed, applying beamforming and DOA estimation algorithms. The estimation error was also calculated, and the results are presented in Tables 5-8.

In accordance with Table 5, the runtime of LCMV algorithm is less significant than any of the direction of arrival algorithms (MUSIC or ESPRIT), and a variation with SNR is not significantly noted when SNR changes from 10 to 15 dB, although approximately doubles when SNR reduces from 10 to 5 dB. The MUSIC estimation algorithm is temporally extremely heavier than the ESPRIT. Note that the execution times don't have a marked variation with noise, despite the τ_{ESPRIT} tends to diminish when the SNR increase.

In terms of errors in the angle of arrival estimation (θ, ϕ) , this error tends to reduce with increasing of SNR. Using the ESPRIT algorithm is observed the reduction of the errors; however, using the MUSIC algorithm the error is constant. This regular value is a consequence of the choice of the evaluation angle grid of the function P_{MUSIC} , as will see after, whereby must be a compromise between execution time and estimation error.

Table 5: Variation of the runtime and estimation error with SNR using LCMV algorithm

		SNR (dB)			
		5	10	15	
LCMV	MUSIC	τ_{MUSIC} (s)	5.92	6.03	5.34
		τ_{LCMV} (s)	0.0199	0.00089	0.00098
		\mathcal{E}_θ (degrees)	0.302	0.302	0.302
		\mathcal{E}_ϕ (degrees)	0.305	0.305	0.305
	ESPRIT	τ_{ESPRIT} (s)	0.052	0.038	0.013
		τ_{LCMV} (s)	0.0013	0.0011	0.0009
		\mathcal{E}_θ (degrees)	0.08	0.04	0.02
		\mathcal{E}_ϕ (degrees)	0.167	0.141	0.0275

Using the Frost's algorithm, as it is adaptive, it has a runtime which diminishes with the SNR, Table 6. The DOA algorithm's performance remained with characteristics already described about the execution time. The estimation errors in the case of MUSIC continue mainly affected due to the selection of interval in the grid angle to evaluate the equation (1), while in ESPRIT is visible an error reduction with the increasing of SNR.

Table 6: Variation of the runtime and estimation error with SNR using Frost's algorithm

		SNR (dB)			
		5	10	15	
FROST's	MUSIC	τ_{MUSIC} (s)	5.67	5.15	5.53
		$\tau_{Frost's}$ (s)	0.0118	0.0047	0.0007
		\mathcal{E}_θ (degrees)	0.302	0.302	0.302
		\mathcal{E}_ϕ (degrees)	0.305	0.305	0.305
	ESPRIT	τ_{ESPRIT} (s)	0.015	0.0018	0.0077
		$\tau_{Frost's}$ (s)	0.013	0.001	0.00086
		\mathcal{E}_θ (degrees)	0.140	0.042	0.042
		\mathcal{E}_ϕ (degrees)	0.0188	0.014	0.010

With the LMS algorithm, according to the Table 7, the execution time reduces while the value of SNR increases, whereas the MUSIC and ESPRIT algorithms keep on with similar characteristics to the preceding cases. The error also shows a reduction with the increase of SNR.

Finally, the Table 8 shows the analysis of the performance using the RLS algorithm. It is possible to see a pronounced reduction of the runtime when SNR changes from 5 dB to 10 dB. The error follows the expected behavior, with a reduction of its value when the DOA ESPRIT algorithm is employed, with the increase

of SNR. When the MUSIC algorithm is used, the error remains constant.

Table 7: Variation of the runtime and estimation error with SNR using LMS algorithm

		SNR			
		5	10	15	
LMS	MUSIC	τ_{MUSIC} (s)	5.35	5.37	5.46
		τ_{LMS} (s)	0.020	0.007	0.002
		\mathcal{E}_θ (degrees)	0.302	0.302	0.302
		\mathcal{E}_ϕ (degrees)	0.305	0.305	0.305
	ESPRIT	τ_{ESPRIT} (s)	0.0095	0.0012	0.0011
		τ_{LMS} (s)	0.0054	0.0050	0.0046
		\mathcal{E}_θ (degrees)	0.203	0.042	0.02
		\mathcal{E}_ϕ (degrees)	0.090	0.045	0.024

Table 8: Variation of the runtime and estimation error with SNR using the RLS algorithm

		SNR			
		5	10	15	
RLS	MUSIC	τ_{MUSIC} (s)	5.82	5.75	5.71
		τ_{RLS} (s)	0.0163	0.0070	0.0161
		\mathcal{E}_θ (degrees)	0.302	0.302	0.302
		\mathcal{E}_ϕ (degrees)	0.305	0.305	0.305
	ESPRIT	τ_{ESPRIT} (s)	0.00181	0.00180	0.0015
		τ_{RLS} (s)	0.0101	0.01	0.01
		\mathcal{E}_θ (degrees)	0.2294	0.0378	0.0972
		\mathcal{E}_ϕ (degrees)	0.156	0.031	0.01

Globally, is noted that the tendency related to beamforming algorithms is the increase of its execution times from the statistically optimum to each of the adaptive ones. The DOA algorithms present consistent results, with a reduction of estimation error with the increase of SNR, taking into account that with MUSIC algorithm a compromise between error and runtime must be done.

Using a considerable number of experiments, a statistical analysis of this performance of each algorithm can be done. This estimate was based on a sequence of 50 experiments, and the graphical analysis is performed in the next figures.

The Fig. 14 shows the runtime of the LCMV algorithm over the number of the n experiments. Despite a couple of experiments presents a more accentuated variation, the mean execution time is about 6.2×10^{-4} seconds (0.62 msec).

The Frost's algorithm execution time is displayed in

the Fig. 15. This algorithm presents a mean value of the 5×10^{-4} seconds (0.5 msec), that although is an adaptive algorithm presents a better result than the previous one.

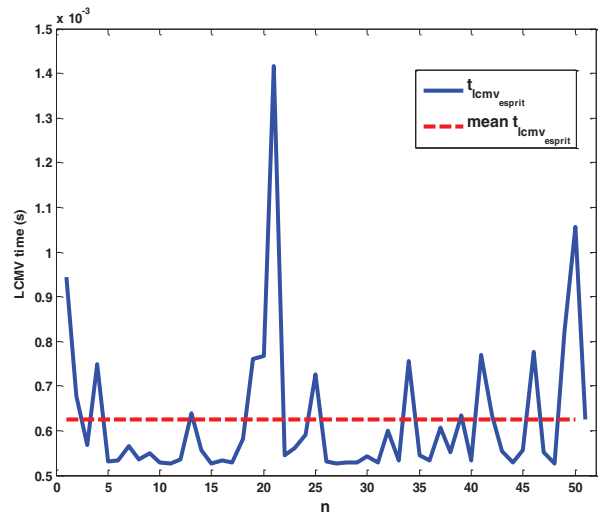


Fig. 14. Execution time of LCMV algorithm.

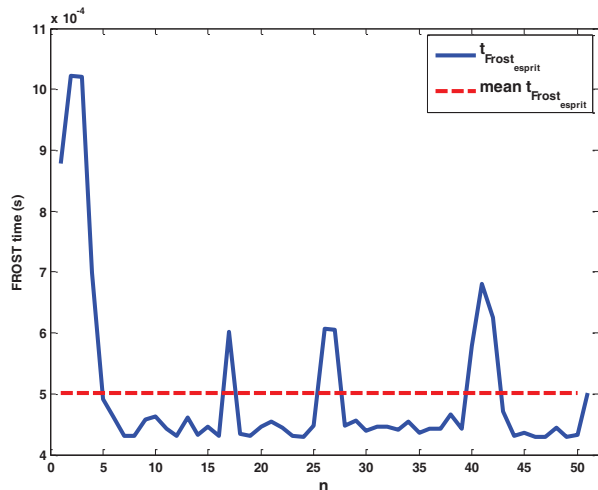


Fig. 15. Execution time of Frost's algorithm.

Using the LMS and RLS algorithms, the used runtime over the experiences are indicated in the Fig. 16 and Fig. 17. The execution times are respectively 2.8×10^{-3} seconds (2.8 msec) and 7.6×10^{-3} seconds (7.6 msec).

Along the n experiences, the runtimes of the two DOA estimation algorithms are displayed in graphical form in the Fig. 18. The upper part includes the values relating to the MUSIC algorithm, while the lower part is concerning to the ESPRIT algorithm. In both the graphs are identified the line of the average time of the various

samples.

Immediately, it is possible to note the huge difference in the time it takes to perform the MUSIC algorithm compared with the ESPRIT. The MUSIC algorithm takes n samples during 5 to 6 seconds each one, presenting an average execution time of 5.54 seconds as shown in Fig. 18. Much less time requires the ESPRIT algorithm, ranging between 1 and 2 milliseconds as the figure shows, with an only sample with a peak reaching 3.5 msec, and the overall average execution time 1.57 msec.

The last parameter that is possible to examine is the estimation error, between the real coordinates (θ, φ) of the incoming waves, and the estimated position determined by the two dimensional DOA algorithms, MUSIC and ESPRIT.

In the Fig. 19, there are exposed the evolution of the estimating error over the n experiences. The superior graph is relating to the coordinate θ , while the bottom is about the φ . In each parts are present the error using the two algorithms of DOA, and further the line of mean of the error. As is possible to see, using the MUSIC algorithm the estimation error have a constant effect, with a mean error of 0.302° in theta and 0.3052° in phi. The ESPRIT algorithm present mean errors much lower, of 0.037° in theta and 0.015° in phi coordinates.

The ESPRIT error is due to the mathematical process and the noise added to the signal. On the other hand, the MUSIC error is strongly due the evaluation interval, as explained in the Fig. 20. The accuracy depends on the number of points on its angle grid, more points lead to longer computations. This is the main issue of MUSIC, and the number of points must be a compromise depending on the required accuracy and computational load.

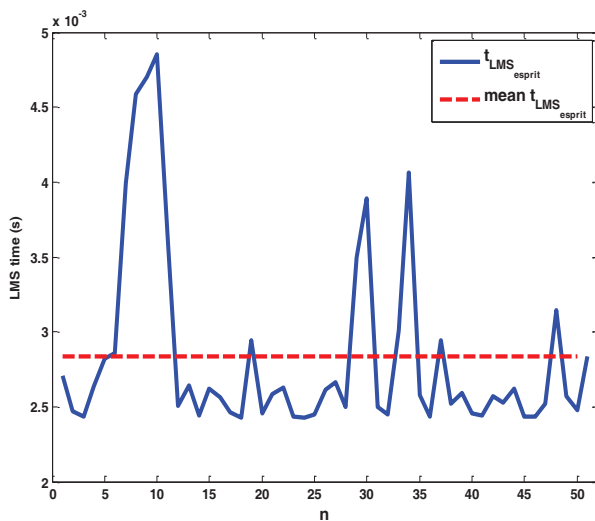


Fig. 16. Execution time of LMS algorithm.

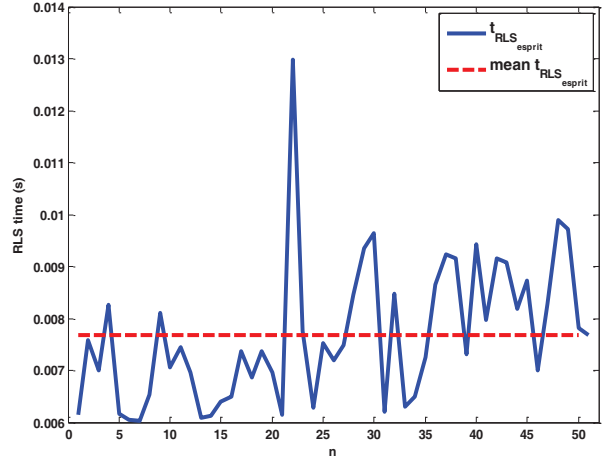


Fig. 17. Execution time of RLS algorithm.

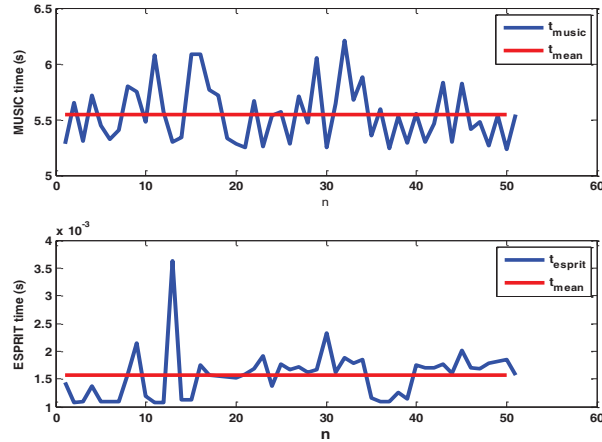


Fig. 18. Execution time evolution of DOA algorithms over n samples.

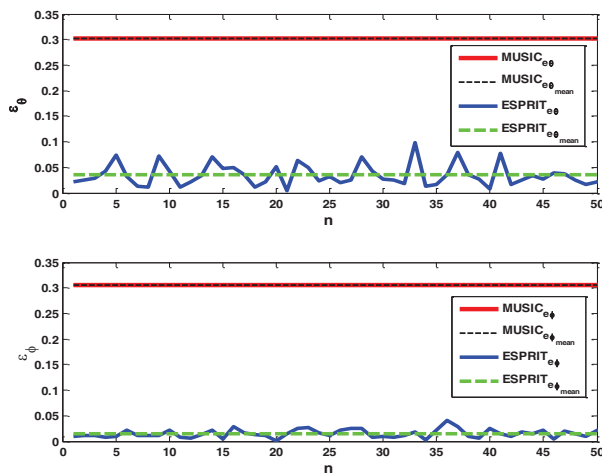


Fig. 19. Estimation error in theta and phi coordinates using each one of DOA algorithms (MUSIC and ESPRIT).

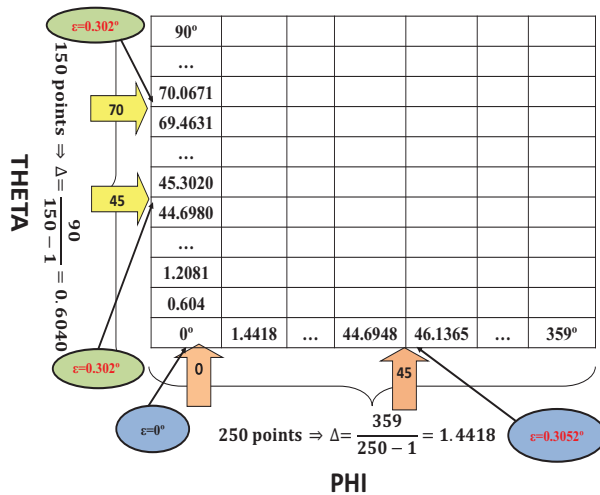


Fig. 20. Evaluation grid of MUSIC algorithm.

VI. DISCUSSION AND FUTURE PROSPECTS

In this paper, the analysis of the main 2D algorithms that are vital in a planar adaptive antenna system, the direction of arrival and the beamforming algorithms, was made.

The developed function to extract the peaks of the MUSIC spectrum is very effective, allowing a correct definition of the maxima values, and the corresponding DOAs. In this work, the weights resulting of the beamforming algorithms, in terms of amplitude and phase, were tested in a simulated array. The intention was to verify that the achieved radiation patterns in electromagnetic simulator present the desired radiation characteristics. About the performance of the algorithms, the runtime of the DOA MUSIC is much higher than ESPRIT, since the MUSIC algorithm must evaluate the MUSIC function to each possible steering vector.

Also about estimating errors, the MUSIC presents some limitations, since the accuracy of the angle results of the interval of evaluating the function. A compromise between the accuracy and the processing time is needed. This fact is something important that is not addressed in [24], so it's a tradeoff to consider. In both DOA algorithms, this error reduces with the increasing of the SNR. The runtime of the beamforming algorithms increases more in the adaptive due to the number of snapshots processed.

The trends involve the use of new, and more complex array topologies, such as three-dimensional arrays, investing in the research of new techniques for determining the DOA's, adapted to them, such as in [25]. Furthermore, advances in beamforming techniques for randomly distributed planar arrays [26], [27] have showed an increased interest, with several applications, either in small satellites or in arrays of sensors, with a non-uniform distribution. Also, is expected the use of smart

antennas in the 5th generation of mobile wireless systems (5G) using MIMO, in the millimeter wave frequencies.

ACKNOWLEDGMENT

This work is funded by National Funds through FCT-Fundação para a Ciência e a Tecnologia under the project PEst-OE/EEI/LA0008/2013.

REFERENCES

- [1] J. Foutz, et. al., *Narrowband Direction of Arrival Estimation for Antenna Arrays*, Morgan & Claypool Publishers, 2008.
- [2] L. C. Godara, "Application of antenna arrays to mobile communications, II. beam-forming and direction-of-arrival considerations," *Proceedings of the IEEE*, vol. 85, no. 8, pp. 1195-1245, Aug. 1997.
- [3] R. O. Schmidt, "Multiple emitter location and signal parameter estimation," *IEEE Transactions on Antennas and Propagation*, vol. 34, no. 3, pp. 276-280, Mar. 1986.
- [4] S. Sekizawa, "Estimation of arrival directions using MUSIC algorithm with a planar array," *IEEE International Conference on Universal Personal Communications, ICUPC '98*, vol. 1, pp. 555-559, Oct. 1998.
- [5] K. V. Rangarao and S. Venkatanarasimhan, "Gold-MUSIC: a variation on MUSIC to accurately determine peaks of the spectrum," *IEEE Transactions on Antennas and Propagation*, vol. 61, no. 4, pp. 2263-2268, Apr. 2013.
- [6] C. C. Yeh, J-H. Lee, and Y. Chen, "Estimating two-dimensional angles of arrival in coherent source environment," *IEEE Transactions on Acoustics, Speech and Signal Proc.*, vol. 37, no. 1, pp. 153-155, Jan. 1989.
- [7] Y. Chen, "On spatial smoothing for two-dimensional direction-of-arrival estimation of coherent signals," *IEEE Transactions on Signal Processing*, vol. 45, no. 7, pp. 1689-1696, Jul. 1997.
- [8] Z. Chen, G. Gokeda, and Y. Yu, *Introduction to Direction-of-Arrival Estimation*, Artech House, 2010.
- [9] M. Haardt, M. D. Zoltowski, C. P. Mathews, and J. A. Nosseck, "2D unitary ESPRIT for efficient 2D parameter estimation," *International Conference on Acoustics, Speech, and Signal Processing, ICASSP-95*, vol. 3, pp. 2096-2099, 1995.
- [10] M. D. Zoltowski, M. Haardt, and C. P. Mathews, "Closed-form 2-D angle estimation with rectangular arrays in element space or beamspace via unitary ESPRIT," *IEEE Transactions on Signal Processing*, vol. 44, no. 2, pp. 316-328, Feb. 1996.
- [11] Y-Y. Wang and W-W. Chen, "A low complexity 2D-DOA estimation algorithm using signal

- decomposition," *High Speed Intelligent Communication Forum*, pp. 1-4, May 10-11, 2012.
- [12] J. Hui and Y. Gang, "An improved algorithm of ESPRIT for signal DOA estimation," *International Conference on Industrial Control and Electronics Engineering (ICICEE)*, pp. 317-320, Aug. 23-25, 2012.
- [13] B. D. Van Veen and K. M. Buckley, "Beamforming: a versatile approach to spatial filtering," *IEEE ASSP Magazine*, vol. 5, no. 2, pp. 4-24, Apr. 1988.
- [14] W. Liu and S. Weiss, *Wideband Beamforming: Concepts and Techniques*, John Wiley & Sons, 2010.
- [15] F. Huang, W. Sheng, and X. Ma, "Efficient parallel adaptive beamforming algorithm for planar array system," *International Symposium on Antennas, Propagation and EM Theory*, pp. 282-285, Nov. 2-5, 2008.
- [16] J-H. Lee and Y-H. Lee, "Two-dimensional adaptive array beamforming with multiple beam constraints using a generalized sidelobe canceller," *IEEE Transactions on Signal Processing*, vol. 53, no. 9, pp. 3517-3529, Sept. 2005.
- [17] A. M. G. Guerreiro, A. D. D. Neto, and F. A. Lisboa, "Beamforming applied to an adaptive planar array," *IEEE Radio and Wireless Conference, RAWCON 98*, pp. 209-212, Aug. 9-12, 1998.
- [18] S. Razia, T. Hossain, and M. A. Matin, "Performance analysis of adaptive beamforming algorithm for smart antenna system," *Informatics, Electronics & Vision (ICIEV), 2012 International Conference on*, pp. 946-949, May 18-19, 2012.
- [19] S. K. Intiaj, I. S. Misra, and R. Biswas, "Performance comparison of different adaptive beamforming algorithm in smart antennas," *International Conference on Computers and Devices for Communication (CODEC)*, pp. 1-4, Dec. 17-19, 2012.
- [20] S-J. Yu and J-H. Lee, "Design of two-dimensional rectangular array beamformers with partial adaptivity," *IEEE Transactions on Antennas and Propagation*, vol. 45, no. 1, pp. 157-167, Jan. 1997.
- [21] R. Li, C. Rao, L. Dai, and S. Zhao, "Adaptive-adaptive beamforming algorithm of planar array based on one-dimensional auxiliary beam," *International Congress on Image and Signal Processing (CISP)*, vol. 7, pp. 3300-3303, Oct. 16-18, 2010.
- [22] Ansoft High Frequency Structure Simulator (HFSS), User's Guide, ed.: REV1.0, Software ver.: 10.0, Ansoft Corporation, Jun. 21, 2005.
- [23] MATLAB, ver. 7.10.0 (R2010a), The MathWorks Inc., Natick, Massachusetts, 2010.
- [24] O. A. Oumar, M. F. Siyau, T. P. Sattar, "Comparison between MUSIC and ESPRIT direction of arrival estimation algorithms for wireless communication systems," *International Conference on Future Generation Communication Technology*, pp. 99-103, Dec. 12-14, 2012.
- [25] B. Errasti-Alcala and R. Fernandez-Recio, "Meta-heuristic approach for single-snapshot 2D-DOA and frequency estimation: array topologies and performance analysis," *Antennas and Propagation Magazine, IEEE*, vol. 55, no. 1, pp. 222-238, Feb. 2013.
- [26] C. G. Christodoulou, M. Ciaurritz, Y. Tawk, J. Costantine, and S. E. Barbin, "Recent advances in randomly spaced antenna arrays," *European Conference on Antennas and Propagation (EuCAP)*, pp. 732-736, Apr. 6-11, 2014.
- [27] M. Ciaurritz, Y. Tawk, C. G. Christodoulou, and J. Costantine, "Adaptive beamforming for random planar arrays," *Antennas and Propagation Society International Symposium (APSURSI), 2014 IEEE*, pp. 1728-1729, Jul. 6-11, 2014.



Tiago Varum got his Master's degree in Electronic and Telecommunications Engineering from Aveiro University in 2010, and started research activities in Telecommunications Institute. His main interest of research is in vehicular communications (DSRC

systems), antenna design, non-uniform antenna arrays, beam-forming and smart/adaptive antennas. In 2012, he started his doctoral research (for Ph.D.) in Electrical Engineering, at Aveiro University, in the field of adaptive beamforming antennas. During this time, he participated in some projects and published several papers in this field, some for conference proceedings and one for a journal. He has also supported teaching activities in the Department of Electronics, Telecommunications and Informatics (DETI) of Aveiro University.



João N. Matos received his diploma in Electronics and Telecommunications Engineering, from Aveiro University, Portugal, in 1982, Master's degree in Computer Science, from the University of Coimbra, Portugal, in 1989, and Ph.D. degree in Electrical

Engineering in 1995, from Aveiro University, Portugal. From 1982 to 1983 he was with Portugal Telecom Innovation. From 1983 to 1995, he was an Assistant Lecturer at University of Aveiro, and a Professor since

1995. Currently he is an Associate Professor at the same University and a Senior Research Scientist at the Institute of Telecommunications. His main scientific interests are in the development of circuits and systems for wireless power transfer and for ITS (Intelligent Transport Systems). He has authored or co-authored more than 70 papers for international journals and conferences.



Pedro Pinho was born in Vale de Cambra, Portugal in 1974. He received the Licenciado and Master's degrees in Electrical and Telecommunications Engineering, and the Ph.D. degree from the University of Aveiro in 1997, 2000, and 2004 respectively. He is currently a Professor Adjunto at the Department of

Electrical Telecommunications and Computers Engineering in Instituto Superior de Engenharia de Lisboa, in Instituto Politécnico de Lisboa, and a Member of the research staff at the Institute for Telecommunications, Aveiro, Portugal from 1997. His current research interest is in antennas for location systems, reconfigurable antennas and antenna design for passive sensors in non-conventional materials. He has authored or co-authored more than 90 papers for conferences and international journals and 4 book chapters.